

## Characterization of the Branching Structure of the Lung from “Macroscopic” Pressure-Volume Measurements

A. Majumdar,<sup>1,2</sup> A. M. Alencar,<sup>1,2</sup> S. V. Buldyrev,<sup>1</sup> Z. Hantos,<sup>3</sup> H. E. Stanley,<sup>1</sup> and B. Suki<sup>2</sup>

<sup>1</sup>Center for Polymer Studies and Department of Physics, Boston University, Boston, Massachusetts, 02215

<sup>2</sup>Department of Biomedical Engineering, Boston University, Boston, Massachusetts, 02215

<sup>3</sup>Department of Medical Informatics and Engineering, and Institute of Surgical Research, University of Szeged, Hungary

(Received 16 November 2000; published 12 July 2001)

We analyze the problem of fluid flow in a bifurcating structure containing random blockages that can be removed by fluid pressure. We introduce an asymmetric tree model and find that the predicted pressure-volume relation is connected to the distribution  $\Pi(n)$  of the generation number  $n$  of the tree's terminal segments. We use this relation to explore the branching structure of the lung by analyzing experimental pressure-volume data from dog lungs. The  $\Pi(n)$  extracted from the data using the model agrees well with experimental data on the branching structure. We can thus obtain information about the asymmetric structure of the lung from macroscopic, noninvasive pressure-volume measurements.

DOI: 10.1103/PhysRevLett.87.058102

PACS numbers: 87.19.Rr, 87.19.Tt, 87.19.Uv, 87.80.Pa

The problem of fluid flow through bifurcating structures is of considerable current interest [1–7]. However, the case when the structure contains random blockages that can be removed by the fluid pressure has been studied only for the simple case of symmetric branching [7,8]. Here we address the problem of forcing fluid (liquid or gas) through asymmetrically branched media in the presence of random closures. Such systems are often encountered during fluid flow in an organ system, such as circulation of blood or flow of air in the lung, where the pathways can be blocked, leading to potentially lethal situations [9,10]. Here we develop a model of the pressure-volume ( $P$ - $V$ ) curve of the lung, and obtain a surprising connection between lung inflation and branching structure. Specifically, fitting the model to experimental pressure-volume data provides information about a key microscopic property of the airway tree, namely, the distribution of the generation numbers of the tree's terminal segments. Since experiments measuring  $P$ - $V$  curves of an inflating lung are noninvasive, this method provides a way to study “microscopic” branching structures from “macroscopic”  $P$ - $V$  data without the use of invasive techniques.

During expiration, peripheral airways in a diseased lung tend to collapse, blocking the flow of air, if the surface tension of the lining fluid is abnormally high [11]. We assume that the lung is completely degassed and all the airways are blocked at the beginning of the inspiratory cycle. These blockages can be removed during inflation if pressure  $P$  reaches the critical opening threshold of the segment [12,13];  $P$  is slowly increased until all closed segments open.

Since the airways are arranged in a treelike branching structure, the opening of one segment is not possible until all segments connecting it to the root of the tree are open. If the threshold pressure of a daughter segment is smaller than that of its parent, the daughter opens simultaneously with the parent. This mechanism also applies to

subsequent generations, leading to avalanches of opening of airways [14].

The process of airway opening via avalanches has been studied for symmetric binary trees [7,8,14,15]. The volume of inhaled air during inspiration follows a simple power law, and the numerical value of the exponent was shown to be equal to the generation number  $n_0$  of the terminal segments [8],

$$V \propto P^{n_0}. \quad (1)$$

The real lung is asymmetric with many branches missing. Hence, to test the departures from the simple power law behavior of Eq. (1), we experimentally determine the  $P$ - $V$  curves of two isolated dog lung lobes, labeled *A* and *B*. We inflate the lobes through the main bronchus, from the collapsed state to total lobe capacity, at an inflation rate such that the time to regain equilibrium after an airway opens is negligible compared to the total time of inflation. The measured  $P$ - $V$  curves are shown in Fig. 1.

Over 90% of the air volume recruited into a lung is contained in the terminal alveoli (air sacs) [16]. Assuming that all alveoli are identical and inelastic, the volume of air at any pressure is proportional to the number of ventilated alveoli. The alveolar elasticity is significant near the end of the inspiratory cycle, after most air sacs have opened [17]. However, we are interested in the air intake due to the avalanche process, not the elastic expansion, and so we concentrate on the region of the  $P$ - $V$  curves in Fig. 1 below the points of inflection, where the elasticity of the air sacs can be ignored. The curves are normalized such that both the  $P$  and  $V$  at the point of inflection are unity as shown in Fig. 2. Examining the  $P$ - $V$  curve on a log-log scale (Figs. 2c and 2d) we can see that a single power law [Eq. (1)] is not sufficient to describe the data.

Next we develop a model to account for the asymmetric branching of the airway tree. Each air sac is labeled with an index  $k$  going from 1 to  $N$  (the total number of

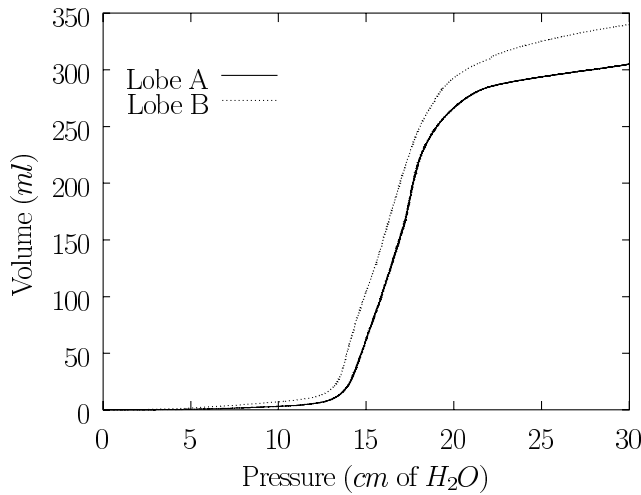


FIG. 1. Experimentally determined  $P$ - $V$  curves of two isolated dog lung lobes  $A$  and  $B$ , obtained during inflation from collapsed state to total lobe capacity, in an inflation time of 120 s. Pressure and airflow are measured using a Valdyne MP-45 transducer and a screen pneumotachometer attached to another Validyne MP-45 transducer, respectively.

air sacs in the lung). The state of being open or closed for each air sac,  $k$ , at pressure  $P$  is then described by a variable  $\sigma_k$  which is  $1/N$  (if the air sac is open) or 0 (if it is closed). We normalize  $\sigma_k$  such that the sum of all  $\sigma_k$  is unity when all air sacs are open. We define the depth,  $n_k$ , for air sac  $k$ , as the number of generations between the air sac and the root of the tree, which is equal to the number

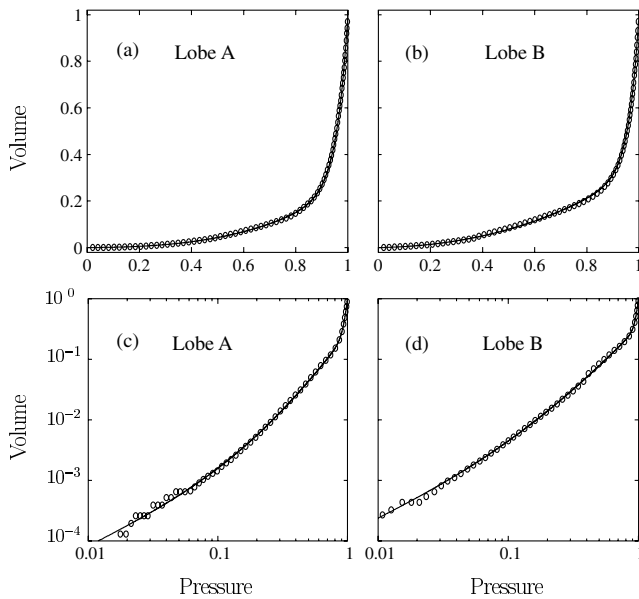


FIG. 2. Pressure-volume data of dog lung lobes, normalized with the inflection point of the curves in Fig. 1 set to (1, 1). The open circles correspond to measured data points, while the solid lines show the curves' fit using Eq. (5). (a) and (b) correspond to the data obtained from two distinct lobes  $A$  and  $B$ . (c) and (d) demonstrate the corresponding fits in a log-log plot, emphasizing the region of small pressures where the small- $n$  part of the distribution  $\Pi(n)$  is dominant.

of blockages that have to be removed to open all segments before the air sac  $k$  can be ventilated. The variable  $\sigma_k$  is dependent upon the threshold pressures of all the segments along this path. Each segment along the path is denoted by a pair of indices  $(j, k)$ , where the index  $k$  identifies the air sac  $k$  it connects and the former index  $j$  describes the number of generations separating the segment from the air sac ( $j = 1, \dots, n_k$ ) [18]. A segment  $(j, k)$  is open only if its threshold pressure,  $T_{jk}$ , is less than the pressure  $P$ . The threshold pressure  $T_{jk}$  of all segments, independent of generation, is drawn from a uniform distribution between 0 and 1 [15,19], a threshold pressure of 1 being the pressure at the inflection point. This amounts to saying that all air sacs are open when  $P$  reaches the inflection point [20]. Since the air sac  $k$  is open only if all segments  $j = 1, \dots, n_k$  are open,  $\sigma_k$  is given by

$$\sigma_k = \frac{1}{N} \prod_{j=1}^{n_k} \Theta(P - T_{jk}), \quad (2)$$

where  $\Theta(x)$  is the unit step function.

To compare our results with experimental data, it is necessary to average over all configurations of threshold pressures  $\{T_{jk}\}$ . The volume,  $V(P)$ , contained in the lung at pressure  $P$  is thus given by the averaged count of all open air sacs,

$$V(P) = \sum_{k=1}^N \langle \sigma_k \rangle, \quad (3)$$

where  $\langle \dots \rangle$  represents an average over all configurations of threshold pressures  $\{T_{jk}\}$ . Using Eq. (2), we obtain

$$\langle \sigma_k \rangle = \frac{1}{N} \prod_{j=1}^{n_k} \int_0^1 dT_{jk} \Theta(P - T_{jk}) = \frac{P^{n_k}}{N}. \quad (4)$$

Equation (4) allows us to express  $\langle \sigma_k \rangle$  in terms of the number of segments along the path from air sac  $k$  to the root of the tree. Thus the branches which are not along this path do not affect the calculation of the average state of air sac  $k$ . Hence the tree is effectively partitioned into a set of  $N$  unbranched pipes. Finally we obtain the averaged volume as a function of inspiratory pressure by using Eqs. (3) and (4),

$$V(P) = \sum_{k=1}^N \frac{P^{n_k}}{N} = \sum_n \Pi(n) P^n, \quad (5)$$

where  $\Pi(n)$  is the fraction of air sacs with depth  $n$ , i.e., the distribution of generation number of the terminal segments.

The expression Eq. (5) for the volume,  $V(P)$ , is a polynomial containing different powers of  $P$ , unlike the result for a symmetric tree in Eq. (1) where a unique exponent corresponds to the single depth  $n_0$ . The result of Eq. (1) can be recovered from Eq. (5) by using  $\Pi(n) = \delta_{n,n_0}$ . The degree of asymmetry is thus manifested in the width of the distribution  $\Pi(n)$ . We note that Eq. (5) combines the effects of the tree structure, as characterized by the depth distribution  $\Pi(n)$ , and the dynamics, characterized by  $P^n$ .

We fit the experimental data with polynomials of order 48, which is the known maximum depth in a dog lung [16].

The coefficients of the polynomial are constrained such that  $\Pi(n) \geq 0$ , for all  $0 \leq n \leq 48$ , and  $\sum \Pi(n) = 1$ . The large number of coefficients makes simple regression extremely unstable, and we use an additive diagonal term in the coefficient matrix to regularize the results. The raw fit thus obtained is then fine-tuned by randomly updating each coefficient by a small amount and recalculating the fitting errors simultaneously in the normal and logarithmic scales, to ensure the accuracy of the coefficients for small  $n$ . The fitted curves are displayed, both on linear (Figs. 2a and 2b) and log-log scales (Figs. 2c and 2d).

The distributions  $\Pi(n)$  thus obtained (Fig. 3) have two distinct regions, a narrow peak for  $n < 5$  and a broad distribution for  $15 < n < 40$ . The terms in the first region contribute to the  $P$ - $V$  curve at small  $P$  when very few air sacs are ventilated (Figs. 2c and 2d). The second part of the distribution has two main peaks in the region  $22 < n < 30$ .

We compare  $\Pi(n)$  to a known model for the airway tree structure, the Horsfield model [16] which is an asymmetric self-similar description of averaged experimental data obtained by physical measurements on a polymer cast of the airway tree. The small- $n$  part of the distribution ( $n < 5$ ) that we obtain from our data does not correspond to the branching structure of the tree since the Horsfield model does not have terminals with depths  $n < 13$  (Fig. 3). We attribute the existence of the small- $n$  part of  $\Pi(n)$  to the airway wall elasticity and the volume of air contained in the airways before any air sacs open. The first few segments of the airway tree are held open by cartilaginous rings, and the expansion of these segments at low  $P$  also contributes to the small- $n$  part of  $\Pi(n)$ . We ignore this region when focusing on the branching structure and normalize the Horsfield model to only the area under the second part of the distribution. This normalized distribution obtained using the Horsfield model is shown as a solid line in Fig. 3.

The Horsfield distribution corresponds in shape and position with the  $\Pi(n)$  obtained by fitting the  $P$ - $V$  data. We are also able to recover the two main peaks at approximately their correct positions. However, the Horsfield model is just a simple and idealized description of the dog lung. In contrast, with our approach we can also identify the variation in structure among specific samples as can be seen in the differences between the distributions for lobes  $A$  and  $B$  in Fig. 3.

The estimated distributions fall off faster than the Horsfield model in the region of higher  $n$  due, we believe, to an underestimation of the maximum threshold pressure, i.e., the pressure at which all airways are opened. Our assumption that the maximum threshold pressure of the segments correspond to the pressure at the point of inflection is true when the distribution of threshold pressures is uniform and generation independent [20]. However, if the threshold pressures are generation dependent, the point of inflection underestimates the maximum threshold pressure

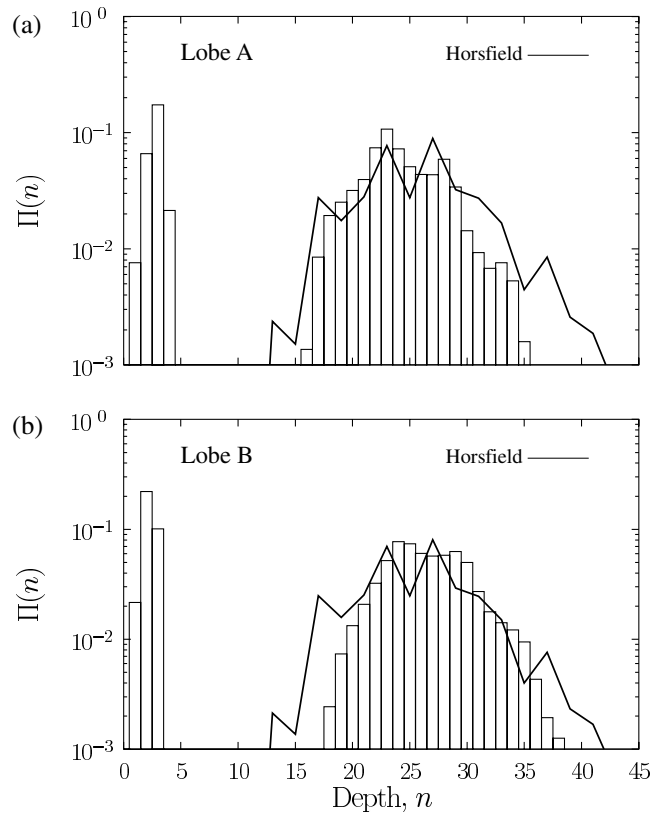


FIG. 3. Distributions of air sac depths,  $\Pi(n)$ , obtained by fitting the  $P$ - $V$  data for two dog lung lobes  $A$  and  $B$ , shown in (a) and (b), respectively, using Eq. (5). The solid lines show the distribution from the experimental data of the Horsfield model, normalized to the area under the part of the distribution resulting from the tree branching structure ( $15 < n < 40$ ).

[15,21]. To estimate the effect of generation dependence, we simulated inflation of randomly branched trees using a simple generation dependent threshold pressure distribution with overlapping domains. We found that the inflection point shifts to a pressure smaller than the maximum threshold pressure, independent of the exact distribution or the degree of randomness in branching. We thus ignore a region of the  $P$ - $V$  curve where the dynamic process of airway opening is still active. The high pressure in this region would allow a more significant contribution from the opening of the deeper air sacs [Eq. (5)], which we are unable to probe accurately. However, in real lungs, these air sacs ( $n > 30$ ) are few in number (Fig. 3) and do not contribute significantly to the shape of the  $P$ - $V$  curve.

The elasticity of the air sacs can also affect the obtained distribution  $\Pi(n)$ . The elastic volume of each air sac  $V_E$  is described by  $V_E(P) = \alpha - \beta e^{-\gamma P}$ , where  $\alpha$ ,  $\beta$ , and  $\gamma$  are parameters determined by fitting experimental data [22]. We expand  $V_E(P) = \sum_{m=0}^{\infty} C_m P^m$ , where  $C_m$  are functions of  $\alpha$ ,  $\beta$ , and  $\gamma$ . The measured volume is now given by the product of the fraction of open air sacs,  $\sum_n \Pi(n) P^n$ , and the elastic volume of each air sac,  $V_E$ . Equation (5) is then replaced by the expression  $V(P) = \sum_{n=1}^{\infty} \Gamma(n) P^n$ , where  $\Gamma_n = \sum_{m=0}^{n-1} C_m \Pi(n-m)$ . Thus

the coefficients of expansion  $\Gamma_n$  of the  $P$ - $V$  relationship are a convolution of the relative frequencies of terminal generation numbers  $\Pi(n)$  and the coefficients of expansion of the elastic term  $C_m$ . Using literature values of  $\alpha$ ,  $\beta$ , and  $\gamma$  [22], we find that the effect of elasticity on the estimated structure is minimal.

In summary, in this paper we introduce a statistical mechanical model of fluid flow through a bifurcating structure in the presence of random blockages that are removed by fluid pressure. When applied to the  $P$ - $V$  curve of the lung, the model allows us to estimate the terminal structure of the airway tree from global noninvasive measurements made at the top of the tree. We note that conventionally, the  $P$ - $V$  curve has been interpreted as a measure of the elastic properties of the lung tissue. Here we take advantage of the fact that fluid blockages have a profound influence on the characteristics of the  $P$ - $V$  curve which allows us to extract structure from data. Since the estimated structure compares favorably to available morphological data, our approach should be useful in clinical situations as well as in developmental studies. This approach should also be applicable to other asymmetrically branched biological and physical systems.

This study was supported by NSF (BES-9813599) and Hungarian Scientific Research Fund Grant No. OTKA T 30670.

- 
- [1] M. F. Shlesinger and B. J. West, Phys. Rev. Lett. **67**, 2106 (1991).
- [2] P. M. Adler, *Porous Media: Geometry and Transport* (Butterworth-Heinemann, Stoneham, MA, 1992).
- [3] H. J. Herrmann, Phys. Rep. **136**, 153 (1986).
- [4] T. Vicsek, *Fractal Growth Phenomena* (World Scientific, Singapore, 1989); *Fractals in Natural Sciences*, edited by T. Vicsek, M. Shlesinger, and M. Matsushita (World Scientific, Singapore, 1994).
- [5] H. Takayasu, *Fractals in the Physical Sciences* (Manchester University Press, Manchester, 1990); *Fractals and Disordered Systems*, edited by A. Bunde and S. Havlin (Springer, Berlin, 1996), 2nd ed.
- [6] J. Andrade, Jr., A. M. Alencar, M. P. Almeida, J. Mendes Filho, S. V. Buldyrev, S. Zapperi, H. E. Stanley, and B. Suki, Phys. Rev. Lett. **81**, 926 (1998); M. Almeida, J. S. Andrade, Jr., S. V. Buldyrev, F. S. A. Cavalcante, H. E. Stanley, and B. Suki, Phys. Rev. E **60**, 5486 (1999).
- [7] A.-L. Barabási, S. V. Buldyrev, H. E. Stanley, and B. Suki, Phys. Rev. Lett. **76**, 2192 (1996).
- [8] B. Suki, J. S. Andrade, Jr., M. F. Coughlin, D. Stamenović, H. E. Stanley, M. K. Sujeer, and S. Zapperi, Ann. Biomed. Eng. **26**, 608 (1998).
- [9] R. H. Ingram, Jr. and T. J. Pedley, in *Handbook of Physiology. The Respiratory System. Mechanics of Breathing* (American Physiological Society, Bethesda, 1986).
- [10] D. MacDonald, *Blood Flow in Arteries* (Williams & Wilkins, Baltimore, 1974).
- [11] D. R. Otis, Ph.D. thesis, Massachusetts Institute of Technology, 1995; D. R. Otis, Jr., F. Peták, Z. Hantos, J. J. Fredberg, and R. D. Kamm, J. Appl. Physiol. **80**, 2077 (1996).
- [12] D. Gaver III, R. Samsel, and J. Solway, J. Appl. Physiol. **69**, 74 (1990).
- [13] P. Macklem, D. Proctor, and J. Hogg, Respir. Physiol. **8**, 191 (1970).
- [14] B. Suki, A.-L. Barabási, Z. Hantos, F. Peták, and H. E. Stanley, Nature (London) **368**, 615 (1994).
- [15] M. Sujeer, S. V. Buldyrev, S. Zapperi, J. S. Andrade, Jr., H. E. Stanley, and B. Suki, Phys. Rev. E **56**, 3385 (1997).
- [16] K. Horsfield, W. Kemp, and S. Phillips, J. Appl. Physiol. **52**, 21 (1982).
- [17] H. Bachofen, J. Hildebrandt, and M. Bachofen, J. Appl. Physiol. **29**, 422 (1970).
- [18] As a segment connects more than one air sac, each segment is multiply labeled.
- [19] The threshold pressure  $T_{jk}$  of a segment ( $j, k$ ) is given by  $T_{jk} \propto \gamma_{jk}/d_{jk}$ , where  $\gamma_{jk}$  is the surface tension of the lining fluid in that segment and  $d_{jk}$  is its diameter. Although  $d_{jk}$  decreases with increasing generations, its distributions significantly overlap from generation to generation. Additionally,  $\gamma_{jk}$  appears to be distributed so that it is higher in the upper part of the tree. These two effects make the distribution of  $T_{jk}$  almost uniform and independent of generation.
- [20] It can be shown that for a model with generation independent, uniform threshold pressure distribution and elastic expansion of the open air sacs, the  $P$ - $V$  curve has a discontinuity in slope at the maximum threshold pressure. In real data, however, additional mechanisms smooth this discontinuity to an inflection point.
- [21] B. Jonson, J. C. Richard, C. Straus, J. Mancebo, F. Lemaire, and L. Brochard, Am. J. Resp. Crit. Care. Med. **159**, 1172 (1999).
- [22] P. S. Haber, H. J. H. Colebatch, C. K. Y. Ng, and I. A. Greaves, J. Appl. Physiol. **54**, 837 (1983).